JMEPEG (2012) 21:2670–2674
DOI: 10.1007/s11665-012-0361-6

1059-9495/$19.00

Characteristics of TiNi Shape Memory Foils Fabricated by Double Cathodes Electrochemical Polishing

S.H. Chang and S.K. Wu

(Submitted February 20, 2012; in revised form August 14, 2012)

$Ti_{50}Ni_{50}$ shape memory foil with 25 μm in thickness and having two smooth surfaces can be fabricated by an electrochemical polishing technique. This technique, using double cathode plates, may shorten the polishing time and alleviate the over-etched pitting effect. The grains on the surface of the hot-rolled sheet are elongated along the rolling direction, and those in the center of the electrochemically polished foil are equal-axial with an average grain size of approximately 8.5 μm. Both transformation temperature and enthalpy of the electrochemically polished foils decrease with the decreasing specimen's thickness. The fabricated $Ti_{50}Ni_{50}$ foils possess the advantages of a more uniform chemical composition throughout the specimen, larger grain size, larger foil area, and greater thickness than those of sputtered TiNi thin films and melt-spun TiNi ribbons.

Keywords electrochemical polishing technique, foil, grain size, thickness effect, TiNi shape memory alloys

1. Introduction

TiNi alloys are important shape memory alloys (SMAs) with good shape memory effect (SME) and superelasticity (PE) (Ref 1). TiNi shape memory thin films, ribbons, and foils are candidates for the microactuators and micropump applications in micro-electro-mechanical systems (MEMS) which because of their advantages of large energy output per unit volume per cycle and large surface area, shortens the response time of SME (Ref 2-6). Melt-spinning and sputtering-deposition techniques are to fabricate amorphous and/or crystalline TiNi-based shape memory ribbons and thin films, respectively (Ref 7-15). However, TiNi thin films fabricated by sputtering-deposition typically do not possess optimal SME because their chemical composition varies significantly throughout the films. In addition, introducing abundant defects or dislocations into the thin films during the fabricating process, which deteriorate the SME and PE properties of the films, are inevitable. Compared to the thin films, TiNi ribbons fabricated by a melt-spinning process, typically possess a thickness below 20 μm, exhibit a more conspicuous martensitic transformation and a better SME. However, the dimensions of these shape memory ribbons are mostly restricted (i.e., the melt-spun ribbon has a longer length in meters but its width and thickness are typically restricted), thus their practical applications in MEMS are also limited. Chen and Wu (Ref 16) reported a method of fabricating TiNi foils using a chemical machining technique. Unfortunately, the surface conditions of these chemical-machined TiNi foils are unacceptable and the over-etched pitting is fatal, often causing the foils to fail. Tomus et al. (Ref 17) researched another fabricating method by alternatively stacking pure Ti and Ni thin films followed by annealing at 800 °C for 10 h to produce a TiNi foil. However, the primary disadvantage of this method is that only thick foil, such as 50 μm in thickness, may be achieved. Recently, Wu and Chang (Ref 18) proposed a novel method of fabricating TiNi foils with 25 μm in thickness using an electrochemical polishing technique to thin a TiNi sheet. In this technique, double cathode plates are used during the electrochemical polishing process. The polishing time for fabricating foils may be shortened and fatal over-etched pitting is alleviated. However, the shape memory characteristics of the foils fabricated by this technique have never been studied. Therefore, in this study, the surface morphology and the martensitic transformation of $Ti_{50}Ni_{50}$ foils with different thicknesses fabricated by an electrochemical polishing technique are investigated.

2. Experimental Procedures

The $Ti_{50}Ni_{50}$ foils used in this study were prepared by an electrochemical polishing technique (Ref 18). Pure titanium (purity, 99.7 wt.%) and nickel (purity, 99.9 wt.%) were melted and remelted a minimum of six times in an argon atmosphere by a vacuum arc remelter to form a $Ti_{50}Ni_{50}$ ingot. The $Ti_{50}Ni_{50}$ ingot was approximately $65.4 \times 38.4 \times 10.5$ mm^3 in dimensions and approximately 120 g in weight. The $Ti_{50}Ni_{50}$ ingot was hot-rolled at 900 °C to a plate 1 mm in thickness. The hot-rolled $Ti_{50}Ni_{50}$ plate was

This article is an invited paper selected from presentations at the International Conference on Shape Memory and Superelastic Technologies 2011, held November 6-9, 2011, in Hong Kong, China, and has been expanded from the original presentation.

S.H. Chang, Department of Chemical and Materials Engineering, National I-Lan University, I-Lan 260, Taiwan; and **S.K. Wu**, Department of Materials Science and Engineering, National Taiwan University, Taipei 106, Taiwan. Contact e-mails: shchang@niu.edu.tw and skw@ntu.edu.tw.

cut into several plates of an appropriate size and then hot-rolled into thinner plates with 0.5 mm in thickness. A portion of the hot-rolled $Ti_{50}Ni_{50}$ plates were cut to approximately $50 \times 50 \times 0.5$ mm^3 in size and each of the plates was sandwiched by two stainless steel plates with dimensions similar to those of the $Ti_{50}Ni_{50}$ plate. The sandwiched $Ti_{50}Ni_{50}$ and stainless steel plates were tightly joined by spot welding along the edges of the sandwiched plates. The joined sandwiched plates (approximately 1.5 mm in thickness) were then hot-rolled at 900 °C to approximately 0.7 mm in thickness, from which thinner $Ti_{50}Ni_{50}$ plates with 0.2 mm in thickness were obtained, after removal from the sandwiched plates. Then, each of the $Ti_{50}Ni_{50}$ plates was sandwiched and joined again by another two stainless steel plates with 0.5 mm in thickness and hot-rolled at 900 °C to obtain a thinner $Ti_{50}Ni_{50}$ sheet with a thickness of 0.13 mm. The $Ti_{50}Ni_{50}$ sheet was annealed at 600 °C for 1 h to eliminate the defects and dislocations introduced during the hot-rolling process. The oxide layer on the $Ti_{50}Ni_{50}$ sheet surface was removed by chemical etching with a solution of $HF:HNO_3:H_2O = 1:5:20$ in volume for approximately 6 h without stirring. The $Ti_{50}Ni_{50}$ sheet, after removing the oxide layer, was approximately 100 μm in thickness, possessed a bright surface without scales included in the matrix, and was used for further thinning processes using the electrochemical polishing technique.

Figure 1 shows the schematic diagram of the double cathodes electrochemical polishing apparatus used in this study. The electrolyte used in the electrochemical polishing process was perchloric acid (70% $HClO_3$) and acetic acid (99.8% CH_3COOH) in a volume ratio of 5:100. Two copper plates were used as the cathodes and placed on the two sides parallel to the $Ti_{50}Ni_{50}$ sheet (anode). Two dc rectifiers were used as the power supplies to reduce electrochemical polishing time. The electrochemical polishing process was carried out in an isothermal water bath (25 °C) to prevent temperature change. The electrochemical polishing process was under current control and the applied voltage and current were set at about 20 V and 1 A, respectively. Martensitic transformation temperatures and enthalpies of the acquired $Ti_{50}Ni_{50}$ foils were determined by differential scanning calorimetry (DSC) with the TA Q10 DSC equipment at a constant heating/cooling rate of 10 °C/min. Thickness and surface morphology of the $Ti_{50}Ni_{50}$ foils were observed by a Philip XL 30 scanning electron microscope (SEM).

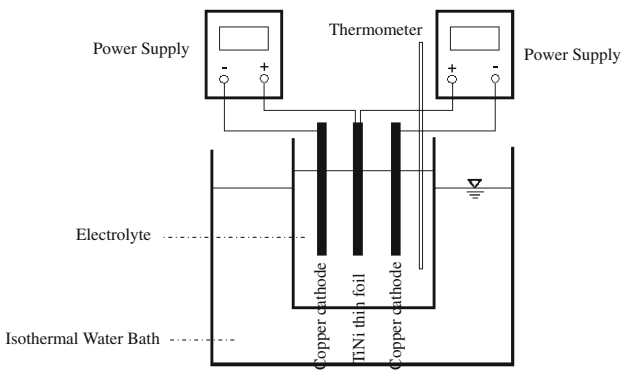

Fig. 1 Schematic diagram of the double cathodes electrochemical polishing apparatus

3. Results

3.1 Thickness Reduction of the Electrochemically Polished $Ti_{50}Ni_{50}$ Foil

Figure 2 plots the thickness of the electrochemically polished $Ti_{50}Ni_{50}$ foil as a function of the electrochemical polishing time. Figure 2 shows that the thickness of the $Ti_{50}Ni_{50}$ foil may be thinned from 100 to 25 μm in 12 min. Here, the $Ti_{50}Ni_{50}$ foil with 100 μm in thickness was electrochemically polished from the hot-rolled $Ti_{50}Ni_{50}$ sheet for several seconds. As shown in Fig. 2, the relationship between the foil thickness and the electrochemical polishing time shows sigmoid characteristics and may be well fitted by a Boltzmann sigmoid decay function with $R^2 = 0.994$. Figure 3 shows the SEM image of the cross-sectional $Ti_{50}Ni_{50}$ foil after electrochemical polishing for 12 min. In Fig. 3, the $Ti_{50}Ni_{50}$ foil shows a uniform thickness of approximately 25 μm with smooth surfaces. The size of the fabricated $Ti_{50}Ni_{50}$ foil with 25 μm in thickness (approximately 30×30 mm^2 in area) is significantly larger than that of the melt-spun ribbon (typically approximately 2 mm in width).

3.2 Surface Morphology of the Electrochemically Polished $Ti_{50}Ni_{50}$ Foil

Figure 4(a) and (b) shows the SEM image of the surface morphology of the $Ti_{50}Ni_{50}$ foil with 100 μm in thickness and that of the same specimen after electrochemically polished to 25 μm in thickness, respectively. Figure 4(a) shows that the grains on the foil surface are elongated along the rolling direction. This is because of the shearing effect caused by the friction between the rollers and the sheet during the hot-rolling process. Figure 4(b) shows that the grains on the surface of the electrochemically polished $Ti_{50}Ni_{50}$ foil are equal-axial with an average grain size of approximately 8.5 μm. The surface morphology of the foil shown in Fig. 4(b) appears significantly more corrugated compared to the cross-sectional image shown in Fig. 3. This feature may be because of the surface relief and the electrochemically polished effects which are more significant on the surface of the foil than at the edge of the foil.

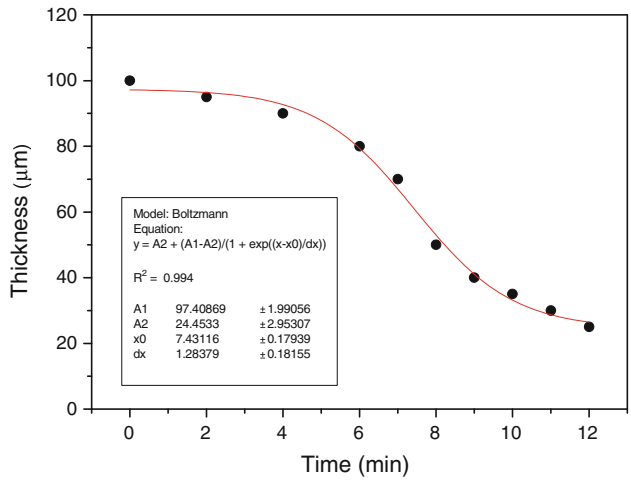

Fig. 2 The thickness of the electrochemically polished $Ti_{50}Ni_{50}$ foil as a function of electrochemical polishing time

3.3 Martensitic Transformation of the Electrochemically Polished $Ti_{50}Ni_{50}$ Foil

Figure 5(a) and (b) shows the cooling and heating DSC curves, respectively, of the electrochemically polished $Ti_{50}Ni_{50}$ foils with different thicknesses. In Fig. 5, each specimen shows a peak associated with B2 → B19′ martensitic transformation in cooling and with B19′ → B2 in heating. Figure 6(a) plots the martensitic transformation peak temperature (M^*) and austenitic transformation peak temperature (A^*), determined from Fig. 5, as a function of the $Ti_{50}Ni_{50}$ foil thickness. In Fig. 6(a), both M^* and A^* temperatures decrease with the decreasing of the specimen's thickness. Figure 6(b) plots the transformation enthalpies of B2 → B19′ transformation peak ($\Delta H(M^*)$) and those of B19′ → B2 one ($\Delta H(M^*)$), shown in Fig. 5, as a function of the specimen's thickness. As shown in Fig. 6(b), the $\Delta H(M^*)$ and $\Delta H(A^*)$ values of the $Ti_{50}Ni_{50}$ foil determined from each specimen are almost identical. Figure 6(b) also shows that both the $\Delta H(M^*)$ and the $\Delta H(A^*)$ values of the $Ti_{50}Ni_{50}$ foil with 100 μm in thickness are comparable to those of the bulk $Ti_{50}Ni_{50}$ SMA (typically ΔH = 25 J/g), but decrease to only ΔH = 10 J/g when the specimen's thickness is 25 μm.

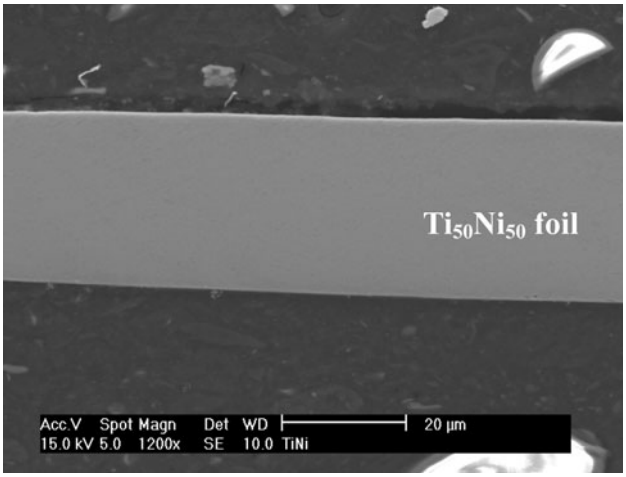

Fig. 3 Cross section SEM images for the electrochemically polished $Ti_{50}Ni_{50}$ foil observed at a magnification of 1,200×

4. Discussion

Thickness measurements shown in Fig. 2 indicate that the method of double cathodes may provide a higher thickness reduction rate than that of the traditional electrochemical polishing using only a single cathode (Ref 16). With prolonging electrochemical polishing time, the thickness of the $Ti_{50}Ni_{50}$ foil may be further reduced, but the lethal over-etched pitting corrosion causes the edge of the foil to be significantly attacked, and leads to the failure of the foil. SEM images show that the grains on the foil surface are elongated along the rolling direction. However, this shearing effect is conspicuous only at the outer surface of the hot-rolled sheet. SEM images also show that the grain size of the electrochemically polished $Ti_{50}Ni_{50}$ foil is similar to that of the TiNi bulk alloys (approximately 10 μm), but is much larger than that of the sputtered thin films (approximately several sub-micrometers) (Ref 6). This feature implies that the electrochemically polished foil may possess better shape memory properties than the sputtered thin film, because TiNi SMAs with ultra-fine grains typically do not exhibit strong shape memory properties (Ref 6).

DSC results show that both the forward and the reverse transformation peaks of the foils become broader and their peak height are lower with the decreasing of the specimen's thickness. This is because the thermal contact resistance and the heat flow delay among the stacked foils become more significant when the stacked foil fragments are put in the DSC pan to obtain sufficient weight for appropriate DSC results. (Ref 19, 20). Kuninori et al. (Ref 21) reported that, for the transmission electron microscope (TEM) specimen, TiNi thin foil with a thickness thinner than approximately 100 nm does not exhibit the martensitic transformation although it was cooled to 98 K. This is because the surface energy of the thin foil strongly depresses the martensitic transformation. Accordingly, the thinner $Ti_{50}Ni_{50}$ foil, possessing a lower transformation temperature may be ascribed to the fact that the surface energy effect is more conspicuous for thinner foil. In addition, the thinner $Ti_{50}Ni_{50}$ foil possesses a lower ΔH value than that of the thicker one. This characteristic may be because the martensitic transformation of thinner foil is depressed more significantly by the surface energy. Compared to other TiNi-based shape memory ribbons, $Ti_{50}Ni_{50}$ foils with 25 μm in thickness possess larger ΔH values than melt-spun and crystallized $Ti_{50}Ni_{25}Cu_{25}$ ribbons with approximately 20 μm

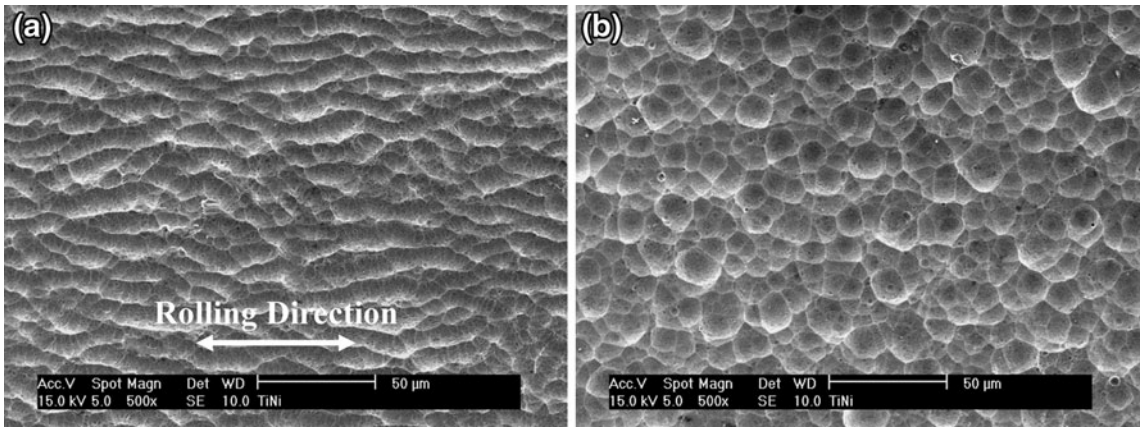

Fig. 4 Surface morphologies of the electrochemically polished $Ti_{50}Ni_{50}$ foil with (a) 100 μm and (b) 25 μm in thickness

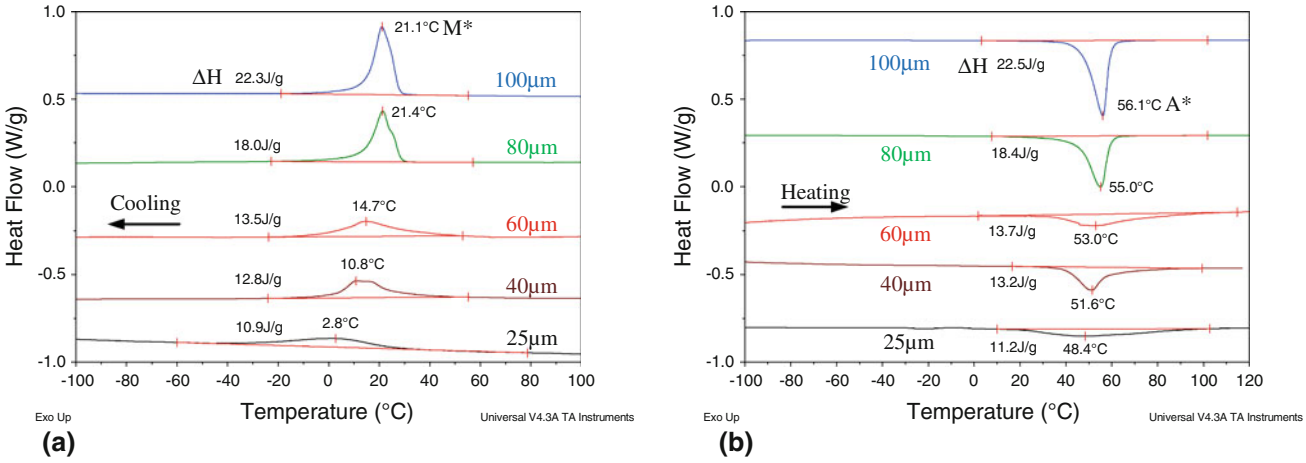

Fig. 5 DSC (a) cooling and (b) heating curves for the electrochemically polished $Ti_{50}Ni_{50}$ foils with different thicknesses

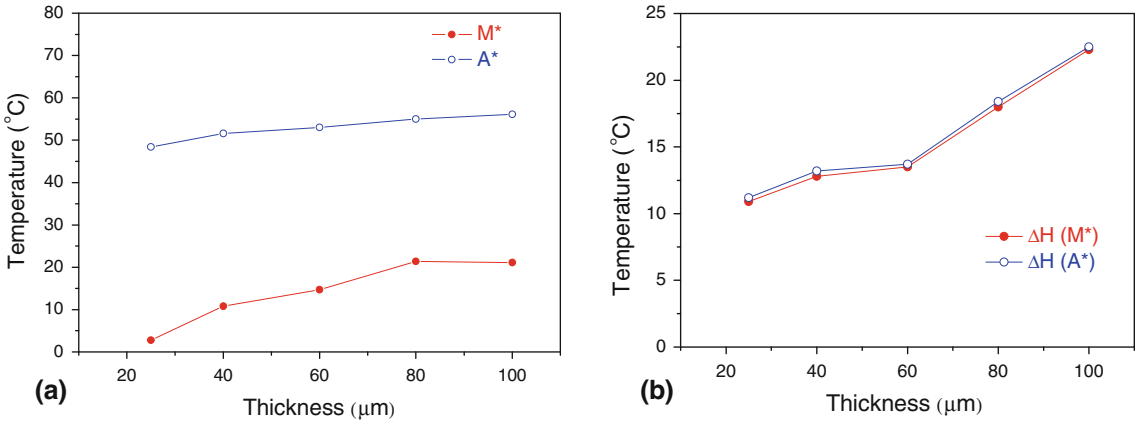

Fig. 6 Evolution of (a) transformation peak temperatures and (b) transformation enthalpies as a function of the specimen thickness for the electrochemically polished $Ti_{50}Ni_{50}$ foils

in thickness (ΔH is below 8 J/g) (Ref 10). This feature implies that the shape memory properties of $Ti_{50}Ni_{50}$ foils fabricated in Fig. 1 could be better than those of the crystallized $Ti_{50}Ni_{25}Cu_{25}$ ribbons. The yield of the $Ti_{50}Ni_{50}$ shape memory foils fabricated by double cathodes electrochemical polishing is not sufficient because more than 75% of the material is wasted when the thickness of the foil is reduced from 100 to 25 μm. However, compared to sputtered TiNi thin films and melt-spun TiNi ribbons, $Ti_{50}Ni_{50}$ foils fabricated by double cathodes electrochemical polishing has the advantages of a more uniform chemical composition throughout the specimen, larger grain size, larger foil area and, greater thickness.

5. Conclusions

The double cathodes electrochemical polishing technique fabricates a $Ti_{50}Ni_{50}$ shape memory foil with 25 μm in thickness, and has smooth and bright surfaces from a $Ti_{50}Ni_{50}$ sheet with 100 μm in thickness. SEM microstructural observations reveal that the grains at the surface of the hot-rolled $Ti_{50}Ni_{50}$ sheet with 100 μm in thickness are elongated along the rolling direction, but those in the center are equal-axial with an average size of approximately 8.5 μm. The martensitic transformation peak in DSC experiments becomes broader and its height is lower when the specimen's thickness decreases, because the surface energy effect becomes more significant in thinner foil. The electrochemically polished $Ti_{50}Ni_{50}$ foils possess the advantages of a more uniform chemical composition throughout the specimen, larger grain size, larger foil area, and greater thickness than those of sputtered TiNi thin films and melt-spun TiNi ribbons.

Acknowledgments

The authors gratefully acknowledge the financial support provided for this research by National Science Council (NSC), Taiwan, Republic of China, under the Grant Nos. NSC100-2221-E002-100-MY3 and NSC-99-2221-E197-010.

References

1. C.M. Wayman and T.W. Duerig, Ni-Ti based shape memory alloys, *Engineering Aspects of Shape Memory Alloys*, T.W. Duerig, K.N. Melton, D. Stöckel, and C.M. Wayman, Ed., Butterworth-Heinemann, London, 1990, p 3–20
2. P. Krulevitch, A.P. Lee, P.B. Ramsey, J.C. Trevino, J. Hamilton, and M.A. Northrup, Thin Film Shape Memory Alloy Microactuators, *J. Microelectromech. Syst.*, 1996, **5**, p 270–282

3. A. Ishida, A. Takei, and S. Miyazaki, Shape Memory Thin Film of TiNi Formed by Sputtering, *Thin Solid Films*, 1993, **228**, p 210–214
4. S. Miyazaki and A. Ishida, Shape Memory Characteristics of Sputter-Deposited Ti-Ni Thin Films, *Mater. Trans., JIM*, 1994, **35**, p 14–19
5. L. Hou and D.S. Grummon, Transformational Superelasticity in Sputtered Titanium-Nickel Thin Films, *Scripta Metall.*, 1995, **33**, p 989–995
6. Y. Fu, H. Du, W. Huang, S. Zhang, and M. Hu, Tini-Based Thin Films in MEMS Applications: A Review, *Sens. Actuatators A*, 2004, **112**, p 395–408
7. Y.W. Kim and T.H. Nam, The Effect of the Melt Spinning Processing Parameters on the Martensitic Transformation in Ti_{50}-Ni_{35}-Cu_{15} Shape Memory Alloys, *Scripta Mater.*, 2004, **51**, p 653–657
8. Y.W. Kim, H.J. Kim, and T.H. Nam, Effect of Annealing Conditions on Microstructures and Shape Memory Characteristics of Ti_{50}-Ni_{30}-Cu_{20} Alloy Ribbons, *J. Alloys Compd.*, 2008, **449**, p 134–138
9. T.H. Nam and Y.W. Kim, Shape Memory Characteristics of Rapidly Solidified $Ti_{50}Ni_{15}Cu_{35}$ Alloy Ribbons, *Intermetallics*, 2010, **18**, p 1946–1949
10. S.H. Chang and S.K. Wu, Annealing Effects on the Crystallization and Shape Memory Effect of $Ti_{50}Ni_{25}Cu_{25}$ Melt-Spun Ribbons, *Intermetallics*, 2007, **15**, p 233–240
11. S.H. Chang, S.K. Wu, and L.M. Wu, Shape Memory Characteristics of As-spun and Annealed $Ti_{51}Ni_{49}$ Crystalline Ribbons, *Intermetallics*, 2010, **18**, p 965–971
12. L.M. Wu, S.H. Chang, and S.K. Wu, Precipitate-Induced R-phase in Martensitic Transformation of As-Spun and Annealed $Ti_{51}Ni_{49}$ Ribbons, *J. Alloys Compd.*, 2010, **505**, p 76–80
13. L.B. Tonga, Y.H. Li, F.L. Meng, H.W. Tian, W.T. Zheng, and Y.M. Wang, Investigation on Mechanical Properties of Sputtered TiNi Thin Films, *J. Alloys Compd.*, 2010, **494**, p 166–168
14. A. Ishida and M. Sato, Microstructures of Crystallized $Ti_{51.5}N_{i48.5}$-xCux (x = 23.4-37.3) Thin Films, *Intermetallics*, 2011, **19**, p 900–907
15. D. König, R. Zarnetta, A. Savan, H. Brunken, and A. Ludwig, Phase Transformation, Structural and Functional Fatigue Properties of Ti-Ni-Hf Shape Memory Thin Films, *Acta Mater.*, 2011, **59**, p 3267–3275
16. J.Z. Chen and S.K. Wu, Chemical Machined Thin Foils of TiNi Shape Memory Alloy, *Mater. Chem. Phys.*, 1999, **58**, p 162–165
17. D. Tomus, K. Tsuchiya, M. Inuzuka, M. Sasaki, D. Imai, T. Ohmori, and M. Umemoto, Fabrication of Shape Memory TiNi Foils via Ti/Ni Ultrafine Laminates, *Scripta Mater.*, 2003, **48**, p 489–494
18. S.K. Wu and S.H. Chang, The Use of Double Cathode Plates Electric Chemical Polishing to Brightening and Thinning Shape Memory Alloys. Taiwan Patent No. I245683, 2005
19. W.W. Wendlandt, *Thermal Analysis*, 3rd ed., Wiley, New York, 1986, p 265
20. J.P. Holman, *Heat Transfer*, 5th ed., McGraw-Hill, New York, 1981, p 48
21. T. Kuninori, E. Sukedai, and H. Hashimoto, Martensitic Transformation in Thin Foil Specimen of a Shape Memory TiNi Alloy, *Mater. Trans., JIM*, 1996, **37**, p 1404–1407